proceedings

MDPI

Proceedings

Optical Properties of Vanadium Oxide/Cellulose Triacetate Photochromic Films †

Joseba Gomez-Hermoso-de-Mendoza [1], Junkal Gutierrez [1,2,*] and Agnieszka Tercjak [1,*]

[1] Group 'Materials + Technologies' (GMT), Department of Chemical and Environmental Engineering, Faculty of Engineering Gipuzkoa, University of the Basque Country (UPV/EHU), Plaza Europa 1, 20018 Donostia-San Sebastian, Spain; joseba.gomezh@ehu.eus

[2] Faculty of Engineering Vitoria-Gasteiz, University of the Basque Country (UPV/EHU), C/Nieves Cano 12, 01006 Vitoria-Gasteiz, Spain

* Correspondence: juncal.gutierrez@ehu.eus (J.G.); agnieszka.tercjaks@ehu.es (A.T.)

† Presented at the First International Conference on "Green" Polymer Materials 2020, 5–25 November 2020; Available online: https://cgpm2020.sciforum.net/.

Published: date

Abstract: The properties of polymer based nanocomposites strongly depend on the fillers added and their dispersion on the matrix. Proposing a simple method that can control these variables is essential to obtain nanocomposites with enhanced properties. In this study, cellulose triacetate based nanocomposites modified with sol-gel synthesised vanadium oxide nanoparticles (V_2O_5) and poly(ethylene oxide-b-propylene oxide-b-ethylene oxide) (PEO-b-PPO-b-PEO or EPE) triblock copolymer were obtained by two methods: solvent casting (SC, drying at ambient conditions) and solvent vapour annealing (SVA, drying under solvent vapour atmosphere). Nanocomposites were characterised by Fourier transform infrared spectroscopy (FTIR) and UV-vis spectroscopy. Nanocomposites presented green colour and high transparency, improving the SVA method the surface finish of the films. Moreover, V_2O_5 nanoparticles provided switchable photochromic properties, changing the film colour from green to pale blue when exposed to UV radiation. Nanocomposites with EPE triblock copolymer presented a more noticeable colour change. As for the speed of the recovery process to the initial state, it increased with the addition of EPE and the sol-gel content. Thus, it was proved that the SVA preparation method was more appropriate that the SC, as well as corroborate that the EPE triblock copolymer and the sol-gel content affected the properties of developed CTA nanocomposites.

Keywords: vanadium oxide; cellulose triacetate; photochromic properties; solvent vapour annealing

1. Introduction

Due to its renewable, sustainable and biodegradable nature [1], cellulose acetate (CA) is one of the most employed polymers even over polycaprolactone (PCL) and polylactide (PLA) [2]. Derived from cotton and wood [3], it presents odourless and non-toxic properties [4], as long as low cost and excellent biocompatibility [5], which make it ideal to cover a wide range of applications from textile, medical and pharmaceutical products to engineering materials, filtration membranes or cigarette filters [6,7], among others.

In order to achieve unique properties of polymeric matrix based nanocomposites, different fillers such as nanoparticles are usually added [8–10]. Moreover, nanostructuration agents like block copolymers are an interesting option to obtain polymeric blends, since their addition is strongly related with their ability to act as nanostructuration agents leading to nanostructured polymers [11].

The choice of the preparation conditions and method employed to obtain the nanocomposites is also crucial, since different factors such as the nanoparticles dispersion, which are influenced by the

preparation conditions, determine the ultimate properties of the nanocomposites. In this way, the solvent evaporation rate and the type of solvent employed in solvent casting can affect the optical properties of cellulose triacetate (CTA) films due to the differences in the movement and molecular orientation of the polymeric chains in the solvent removal [12,13]. In the case of sorption films, the adsorbing capacity to remove dyes of chitosan based nanocomposites can be enhanced dispersing by sonication previously synthesised Fe_3O_4 magnetic nanoparticles into the film forming solution [14] and applying ultrasound to TiO_2 and ZnO nanoparticles [15]. Moreover, the solution method is more effective than melting blending method in the preparation of montmorillonite/thermoplastic starch films, since the mechanical properties improve due to the differences in the water absorption [16].

In this study, cellulose triacetate (CTA) based nanocomposites modified with sol-gel synthesised vanadium oxide nanoparticles (V_2O_5) and poly(ethylene oxide-b-propylene oxide-b-ethylene oxide) (PEO-b-PPO-b-PEO or EPE) triblock copolymer were obtained by solvent casting (SC) and solvent vapour annealing (SVA) preparation methods. On the one hand, the V_2O_5 nanoparticles provided photochromic properties to the obtained nanocomposites. On the other hand, the SVA preparation method enhanced the surface finish of the nanocomposite films. The obtained nanocomposites were analysed by Fourier transform infrared spectroscopy (FTIR) and UV-vis spectroscopy. Photochromic properties were also studied.

2. Experiments

2.1. Materials

Cellulose triacetate (CTA, Mn 50,000 g mol^{-1}, DS 2.92) and poly(ethylene oxide-b-propylene oxide-b-ethylene oxide) triblock copolymer (EPE, Mn 12,600 g mol^{-1}, 70% PEO) were purchased from Sigma Aldrich. Acetic acid and acetone were supplied by Panreac, and isopropanol by Scharlau. Vanadium (V) oxytriisopropoxide ($(OV(OCH(CH_3)_2)_3)$) (VOIT) was provided from Sigma Aldrich and used to obtain the sol-gel synthesised V_2O_5 nanoparticles. All the reagents were employed as received.

2.2. Preparation of Nanocomposites

Cellulose triacetate based nanocomposites modified with V_2O_5 nanoparticles, without and with EPE triblock copolymer and denominated V_2O_5/CTA and V_2O_5-EPE/CTA, respectively, were obtained. Solutions of CTA (1 g) in acetone (25 mL) were prepared, adding EPE (0.1 g) in the case of V_2O_5-EPE/CTA nanocomposites, and stirred for 24 h. Additionally, isopropanol, VOIT and acetic acid were mixed (80:1:1 volume ratio) and stirred for 2 h. After that, sol-gel solution was added in the suitable proportion to CTA and EPE/CTA, obtaining solutions with 1, 3, 5, and 10 vol% of sol-gel (with respect to the initial 25 mL solution) and stirred for 1 h. Finally, nanocomposites were solvent casted employing two different drying conditions. On the one hand, nanocomposites were dried uncontrolled at ambient conditions (SC). On the other hand, films were solvent vapour annealed keeping them under acetone vapour atmosphere in an oven at 25 °C for 1 week (SVA).

2.3. Characterisation

2.3.1. Fourier-Transform Infrared Spectroscopy (FTIR)

Fourier transform infrared (FTIR) spectra were performed using a Nicolet Nexus FTIR spectrometer equipped with a Golden Gate (Specac) ATR sampling accessory. The background was recorded before every sample and the spectra were obtained in the range of 4000–700 cm^{-1} with 32 scans.

2.3.2. UV-Vis Spectroscopy

UV-3600 Shimadzu UV-VIS-NIR spectrophotometer was employed to obtain the transmittance spectra of the nanocomposites within the range of 200−800 nm. Transmittance values at 650 nm were taken as an indicative of nanocomposites transparency. As for the switchable photochromic properties, nanocomposites were firstly irradiated with 254 nm UV light during 5 min using UV lamp (XX-15S UV Bench Lamp, 15 W). The distance between the sample and the source was set in 12 cm. The irradiated samples were then monitored with the spectrophotometer to estimate the time needed to reach the initial state, denominated recovery time.

3. Results and Discussion

3.1. Appearance of Investigated Films

Both SC and SVA nanocomposites presented high flexibility and green colour due to the presence of vanadium oxide nanoparticles [17]. However, nanocomposites prepared by SVA method showed improved surface finish than those prepared by SC, without visible defects and smoother surface. This is due to the SVA method, which allowed a controlled solvent evaporation that affected the surface of the nanocomposites. Moreover, the addition of EPE triblock copolymer darkened the nanocomposites. These differences are reflected in Figure 1, where $5V_2O_5$/CTA and $5V_2O_5$-EPE/CTA nanocomposite films are shown as example.

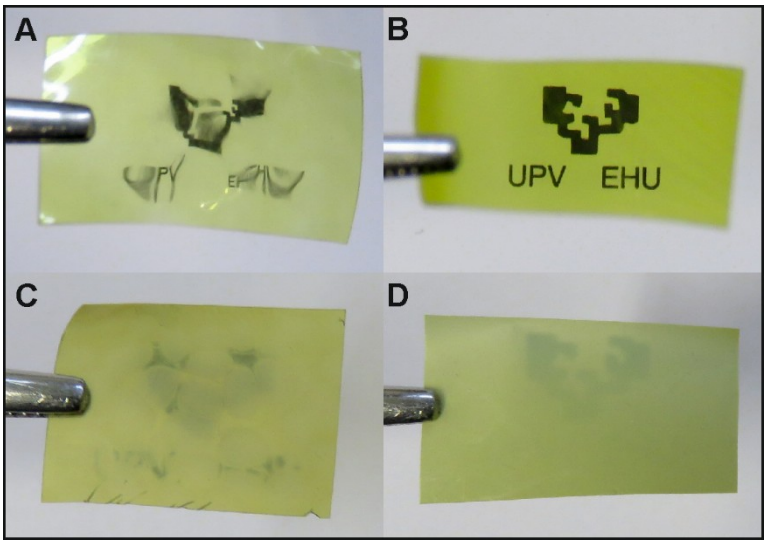

Figure 1. Appearance of $5V_2O_5$/CTA nanocomposite obtained by (**A**) SC and (**B**) SVA and $5V_2O_5$-EPE/CTA nanocomposite obtained by (**C**) SC and (**D**) SVA. Digital images were taken by placing the films at 10 cm from the logo.

Consequently, SVA was presented as an alternative method to obtain micrometre-thick nanocomposite films, being its implementation uncomplicated and providing great improvements in the surface finish. Thus, the employed SVA method would be suitable to scale-up the preparation of films from lab to industry in a simple way. Therefore, it was considered that the SVA method is more appropriate than the SC and in consequence a more comprehensive analysis of SVA nanocomposites was carried out.

3.2. FTIR Characterisation

Figure 2 shows FTIR spectra of (A) V_2O_5/CTA and (B) V_2O_5-EPE/CTA nanocomposites prepared by SVA. All the spectra presented the characteristic bands of CTA: 3500 cm^{-1} (O-H stretching wide band), 2950 and 2900 cm^{-1} (C-H stretching of methoxy group), 1735 cm^{-1} (C=O stretching), 1370 cm^{-1} (C-H stretching), 1215 cm^{-1} (C-O stretching of ether groups) and 1030 cm^{-1} (C-O stretching of OH

groups). Furthermore, as captured in Figure 2, no significant differences were observed in the position of the maximum of these bands of both series of nanocomposites.

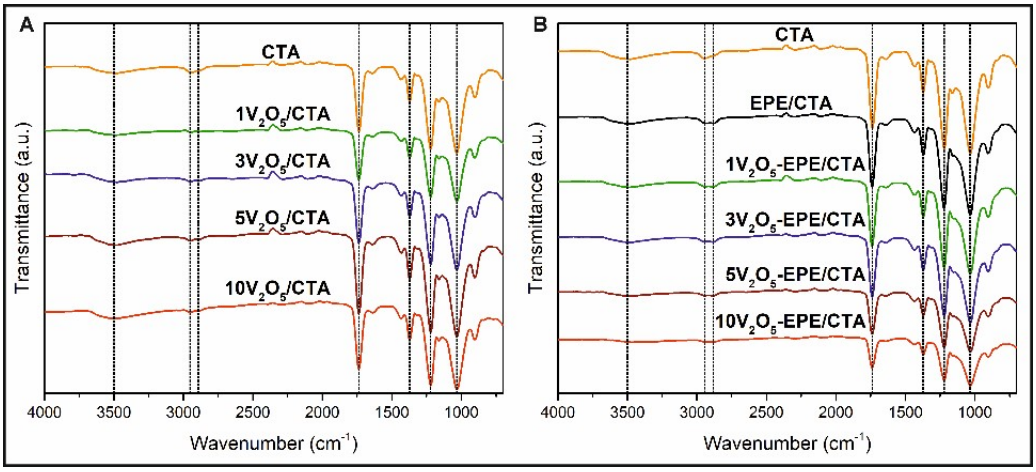

Figure 2. FTIR spectra of (**A**) V_2O_5/CTA and (**B**) V_2O_5-EPE/CTA nanocomposites prepared by SVA.

3.3. UV-Vis Spectra

Figure 3 displays the UV-vis spectra of V_2O_5/CTA and V_2O_5-EPE/CTA nanocomposites prepared by SVA. Transmittance at 650 nm is marked in order to indicate the transparency of the nanocomposites.

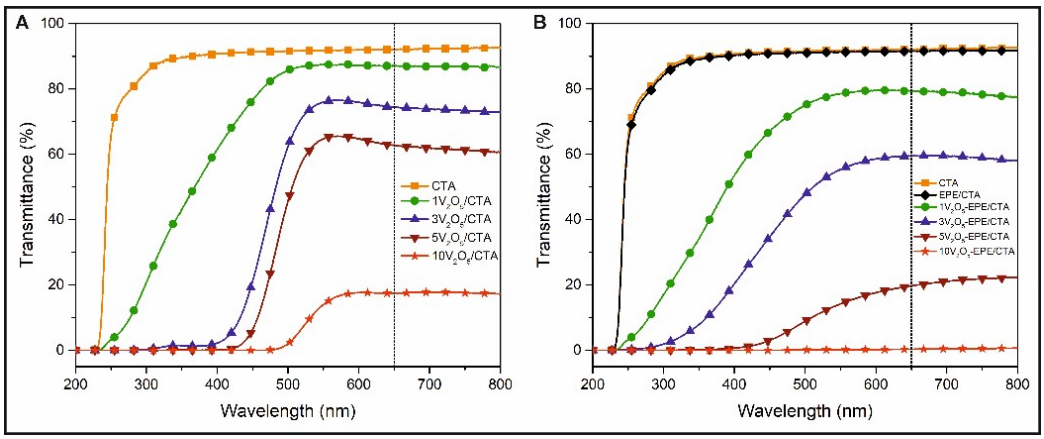

Figure 3. UV-vis spectra of (**A**) V_2O_5/CTA and (**B**) V_2O_5-EPE/CTA nanocomposites prepared by SVA method.

CTA and EPE/CTA presented similar UV-vis curves, both of them with high transparency. Similarly, V_2O_5/CTA and V_2O_5-EPE/CTA nanocomposites displayed also high transparency. However, both series of nanocomposites lost transparency as long as sol-gel content increased. Moreover, V_2O_5-EPE/CTA nanocomposites displayed lower transmittance values than V_2O_5/CTA if compared nanocomposites with the same sol-gel content due to the incorporation of EPE triblock copolymer.

As for the V_2O_5/CTA serie, $3V_2O_5$/CTA, $5V_2O_5$/CTA and $10V_2O_5$/CTA nanocomposites presented transmittance values nearby to 0% until 400, 450 and 500 nm, respectively. This can indicate that these nanocomposites absorb UV radiation, which would protect them from the deterioration caused by it. Nevertheless, only $3V_2O_5$/CTA and $5V_2O_5$/CTA displayed this property with high transparency. On the other hand, in the case of nanocomposites with EPE triblock copolymer, $5V_2O_5$-EPE/CTA and $10V_2O_5$-EPE/CTA presented these UV-shielding properties, although they also showed a decrease in the transparency.

Additionally, photochromic properties of nanocomposites were studied, irradiating them with 254 nm UV light during 5 min. Figure 4 shows the colour change of SVA nanocomposites.

Nanocomposites changed their colour after UV irradiation from light green to pale blue in $1V_2O_5$-EPE/CTA nanocomposite and from light green to darker green in the remaining ones. This blue colour indicated that vanadium presented an oxidation state of +4 [18], as a consequence of a reduction process from +4 to +5 [17,19]. As observed in Figure 4, this colour change was more noticeable in the case of V_2O_5-EPE/CTA nanocomposites, being almost indiscernible for V_2O_5/CTA nanocomposites. As reported by other researchers [20–22], this can be due to the plasticising effect of EPE triblock copolymer. The local environment around the photochromic molecule, which is influenced by free volume, fluidity and polarity, among others, can affect the photochromic response. In this case, the addition of EPE triblock copolymer produced a soft environment, encouraging the molecular mobility, which seemed to help the colouring process of the nanocomposites.

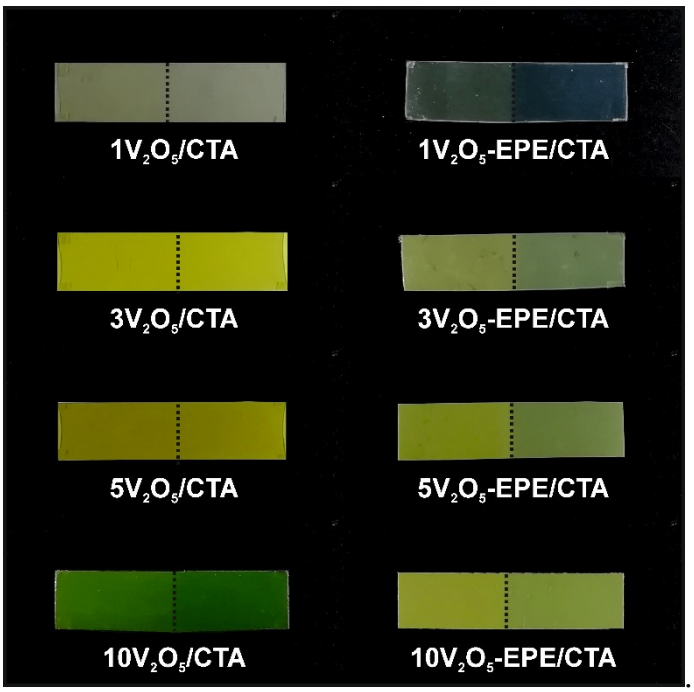

Figure 4. Digital images of V_2O_5/CTA and V_2O_5-EPE/CTA nanocomposites prepared by SVA before (**left** part) and after (**right** part) irradiation.

After a few hours, nanocomposites presented an oxidation process due to the atmospheric oxygen, recovering the initial state and colour as vanadium oxidise from +4 to +5. This process is also influenced by the presence of EPE triblock copolymer and the sol-gel content. In order to perform a thorough analysis, the UV-vis spectra at different times of $1V_2O_5$/CTA, $1V_2O_5$-EPE/CTA and $3V_2O_5$/CTA prepared by SVA were investigated (Figure 5).

$1V_2O_5$/CTA nanocomposite displayed an 88% transmittance value at 650 nm. The irradiation process decreased it to 86%, needing 120 h (5 days) to reach the initial transmittance value. As for $1V_2O_5$-EPE/CTA, it presented a transmittance value of ~78% at 650 nm, decreasing to 75% after the irradiation (0 h). The recovery process was carried out at a higher switching speed than in the case of $1V_2O_5$/CTA nanocomposite, reaching a value of 77%, i.e., a recovery percentage of 83%, at 28 h. It can be said that the initial state was reached after approximately 2 days.

Before the irradiation, $3V_2O_5$/CTA nanocomposite showed a transmittance value of 66% at 650 nm. It decreased to 64% after the irradiation, reaching the initial state after 48 h, a lower recovery time if compared with the 120 h of $1V_2O_5$/CTA nanocomposite. Therefore, it can be said that the switching speed of the recovery process increased as long as sol-gel content increased.

With all the above mentioned, it can be concluded that the addition of EPE triblock copolymer provoked a more effective colouring of the nanocomposites and a higher switching speed of the recovery process. Moreover, it seems that the switching speed increased with the sol-gel content.

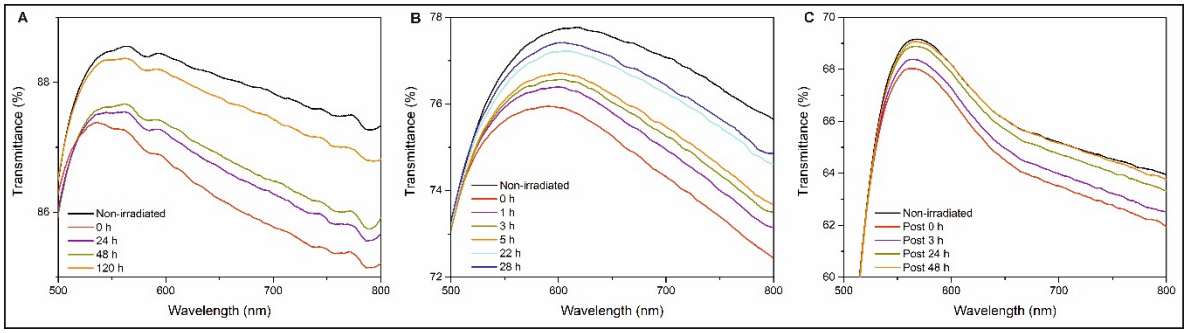

Figure 5. Magnification of UV-vis spectra of (**A**) $1V_2O_5$/CTA, (**B**) $1V_2O_5$-EPE/CTA and (**C**) $3V_2O_5$/CTA nanocomposites prepared by SVA in a function of time before and after irradiation.

4. Conclusions

CTA based nanocomposites were modified with EPE triblock copolymer and sol-gel synthesised V_2O_5 nanoparticles by SC and SVA preparation methods. Both SC and SVA nanocomposites displayed green colour and high flexibility. However, SVA nanocomposites presented smoother surface finish if compared with SC nanocomposites. Moreover, SVA nanocomposites presented high transparency, which decreased with the addition of EPE and the increase of sol-gel content. Additionally, CTA nanocomposites showed switchable photochromic properties when exposed to UV radiation, changing their colour from green to pale blue. This colour change was more noticeable in the nanocomposites with EPE triblock copolymer. In addition, the speed of the recovery process increased with the sol-gel content and the addition of the EPE triblock copolymer. For all the above mentioned, it is demonstrated that the preparation method affects the properties of the developed nanocomposites, being the SVA method more suitable than SC one.

Author Contributions: J.G. and A.T. conceived and designed the experiments; J.G.-H.-d.-M. performed the experiments; J.G., A.T. and J.G.-H.-d.-M. analysed the data; J.G.-H.-d.-M. wrote the paper; J.G. and A.T. reviewed and edited the paper; J.G. and A.T. headed the research. All authors have read and agreed to the published version of the manuscript.

Acknowledgments: Financial support from Spanish Ministry of Science, Innovation and Universities and European Union (MICINN/FEDER and UE) in the frame of PGC2018-097699-B-I00 project and from the Basque Government for PIBA19-0044 project are gratefully acknowledged. Moreover, we are grateful to the Macrobehavior-Mesostructure-Nanotechnology SGIker unit of UPV/EHU. J.G.-H.-de-M. thanks Basque Government for PhD Fellowship (PRE_2020_2_0200).

Conflicts of Interest: The authors declare no conflict of interest. The founding sponsors had no role in the design of the study; in the collection, analyses, or interpretation of data; in the writing of the manuscript, and in the decision to publish the results.

Abbreviations

The following abbreviations are used in this manuscript:

CTA	cellulose triacetate
EPE	poly(ethylene oxide-b-propylene oxide-b-ethylene oxide)
SC	solvent casting
SVA	solvent vapour annealing
VOIT	vanadium (V) oxytriisopropoxide

References

1. Thiangtham, S.; Runt, J.; Manuspiya, H. Sulfonation of dialdehyde cellulose extracted from sugarcane bagasse for synergistically enhanced water solubility. *Carbohydr. Polym.* **2019**, *208*, 314–322, doi:10.1016/j.carbpol.2018.12.080.

2. Huang, H.; Dean, D. 3-D printed porous cellulose acetate tissue scaffolds for additive manufacturing. *Addit. Manuf.* **2020**, *31*, 100927, doi:10.1016/j.addma.2019.100927.
3. Cheng, H.; Dowd, M.K.; Selling, G.; Biswas, A. Synthesis of cellulose acetate from cotton byproducts. *Carbohydr. Polym.* **2010**, *80*, 449–452, doi:10.1016/j.carbpol.2009.11.048.
4. Marrez, D.A.; Abdelhamid, A.E.; Darwesh, O.M. Eco-friendly cellulose acetate green synthesized silver nano-composite as antibacterial packaging system for food safety. *Food Packag. Shelf Life* **2019**, *20*, 100302, doi:10.1016/j.fpsl.2019.100302.
5. Yang, S.; Wang, T.; Tang, R.; Yan, Q.; Tian, W.; Zhang, L. Enhanced permeability, mechanical and antibacterial properties of cellulose acetate ultrafiltration membranes incorporated with lignocellulose nanofibrils. *Int. J. Biol. Macromol.* **2020**, *151*, 159–167, doi:10.1016/j.ijbiomac.2020.02.124.
6. Charvet, A.; Vergelati, C.; Long, D.R. Mechanical and ultimate properties of injection molded cellulose acetate/plasticizer materials. *Carbohydr. Polym.* **2019**, *204*, 182–189, doi:10.1016/j.carbpol.2018.10.013.
7. Das, A.M.; Ali, A.A.; Hazarika, M.P. Synthesis and characterization of cellulose acetate from rice husk: Eco-friendly condition. *Carbohydr. Polym.* **2014**, *112*, 342–349, doi:10.1016/j.carbpol.2014.06.006.
8. Kaya, G.G.; Deveci, H. Synergistic effects of silica aerogels/xerogels on properties of polymer composites: A review. *J. Ind. Eng. Chem.* **2020**, *89*, 13–27, doi:10.1016/j.jiec.2020.05.019.
9. Loste, J.; Lopez-Cuesta, J.-M.; Billon, L.; Garay, H.; Save, M. Transparent polymer nanocomposites: An overview on their synthesis and advanced properties. *Prog. Polym. Sci.* **2019**, *89*, 133–158, doi:10.1016/j.progpolymsci.2018.10.003.
10. Kumar, H.; Kumari, N.; Sharma, R. Nanocomposites (conducting polymer and nanoparticles) based electrochemical biosensor for the detection of environment pollutant: Its issues and challenges. *Environ. Impact Assess. Rev.* **2020**, *85*, 106438, doi:10.1016/j.eiar.2020.106438.
11. Leibler, L. Nanostructured plastics: Joys of self-assembling. *Prog. Polym. Sci.* **2005**, *30*, 898–914, doi:10.1016/j.progpolymsci.2005.06.007.
12. An, M.; Zhang, Q.; Ye, K.; Lin, Y.; Wang, D.; Chen, W.; Yin, P.; Meng, L.; Li, L. Structural evolution of cellulose triacetate film during stretching deformation: An in-situ synchrotron radiation wide-angle X-Ray scattering study. *Polymer* **2019**, *182*, 121815, doi:10.1016/j.polymer.2019.121815.
13. Songsurang, K.; Miyagawa, A.; Manaf, M.E.A.; Phulkerd, P.; Nobukawa, S.; Yamaguchi, M. Optical anisotropy in solution-cast film of cellulose triacetate. *Cellulose* **2013**, *20*, 83–96, doi:10.1007/s10570-012-9807-0.
14. Kloster, G.A.; Mosiewicki, M.A.; Marcovich, N.E. Chitosan/iron oxide nanocomposite films: Effect of the composition and preparation methods on the adsorption of congo red. *Carbohydr. Polym.* **2019**, *221*, 186–194, doi:10.1016/j.carbpol.2019.05.089.
15. Bhanvase, B.A.; Veer, A.; Shirsath, S.; Sonawane, S. Ultrasound assisted preparation, characterization and adsorption study of ternary chitosan-ZnO-TiO2 nanocomposite: Advantage over conventional method. *Ultrason. Sonochem.* **2018**, *52*, 120–130, doi:10.1016/j.ultsonch.2018.11.003.
16. Muller, P.; Kapin, Éva; Fekete, E. Effects of preparation methods on the structure and mechanical properties of wet conditioned starch/montmorillonite nanocomposite films. *Carbohydr. Polym.* **2014**, *113*, 569–576, doi:10.1016/j.carbpol.2014.07.054.
17. Kang, M.; Oh, E.; Kim, I.; Kim, S.W.; Ryu, J.-W.; Kim, Y.-G. Optical characteristics of amorphous V2O5 thin films colored by an excimer laser. *Curr. Appl. Phys.* **2012**, *12*, 489–493, doi:10.1016/j.cap.2011.08.007.
18. Kwon, J.; Fatimah, S.; Baek, S.; Kim, Y.; Yang, H.; Ko, Y. Electrochemical response of VxOy-Al2O3 composite layer with dark-green color achieved by plasma electrolytic oxidation. *J. Alloy. Compd.* **2020**, *827*, 154367, doi:10.1016/j.jallcom.2020.154367.
19. Sajitha, S.; Aparna, U.; Deb, B. Ultra-Thin Manganese Dioxide-Encrusted Vanadium Pentoxide Nanowire Mats for Electrochromic Energy Storage Applications. *Adv. Mater. Interfaces* **2019**, *6*, doi:10.1002/admi.201901038.
20. Such, G.K.; Evans, R.A.; Davis, T.P. Rapid Photochromic Switching in a Rigid Polymer Matrix Using Living Radical Polymerization. *Macromol.* **2006**, *39*, 1391–1396, doi:10.1021/ma052002f.
21. Malic, N.; Campbell, J.A.; Ali, A.S.; York, M.; D'Souza, A.; Evans, R.A. Controlling Molecular Mobility in Polymer Matrices: Synchronizing Switching Speeds of Multiple Photochromic Dyes. *Macromol.* **2010**, *43*, 8488–8501, doi:10.1021/ma101051m.

22. Ratner, J.; Kahana, N.; Warshawsky, A.; Krongauz, V. Photochromic Polysulfones. 2. Photochromic Properties of Polymeric Polysulfone Carrying Pendant Spiropyran and Spirooxazine Groups. *Ind. Eng. Chem. Res.* **1996**, *35*, 1307–1315, doi:10.1021/ie950301v.

.